Unique Properties of Daily Proton Fluxes up to 100 GV

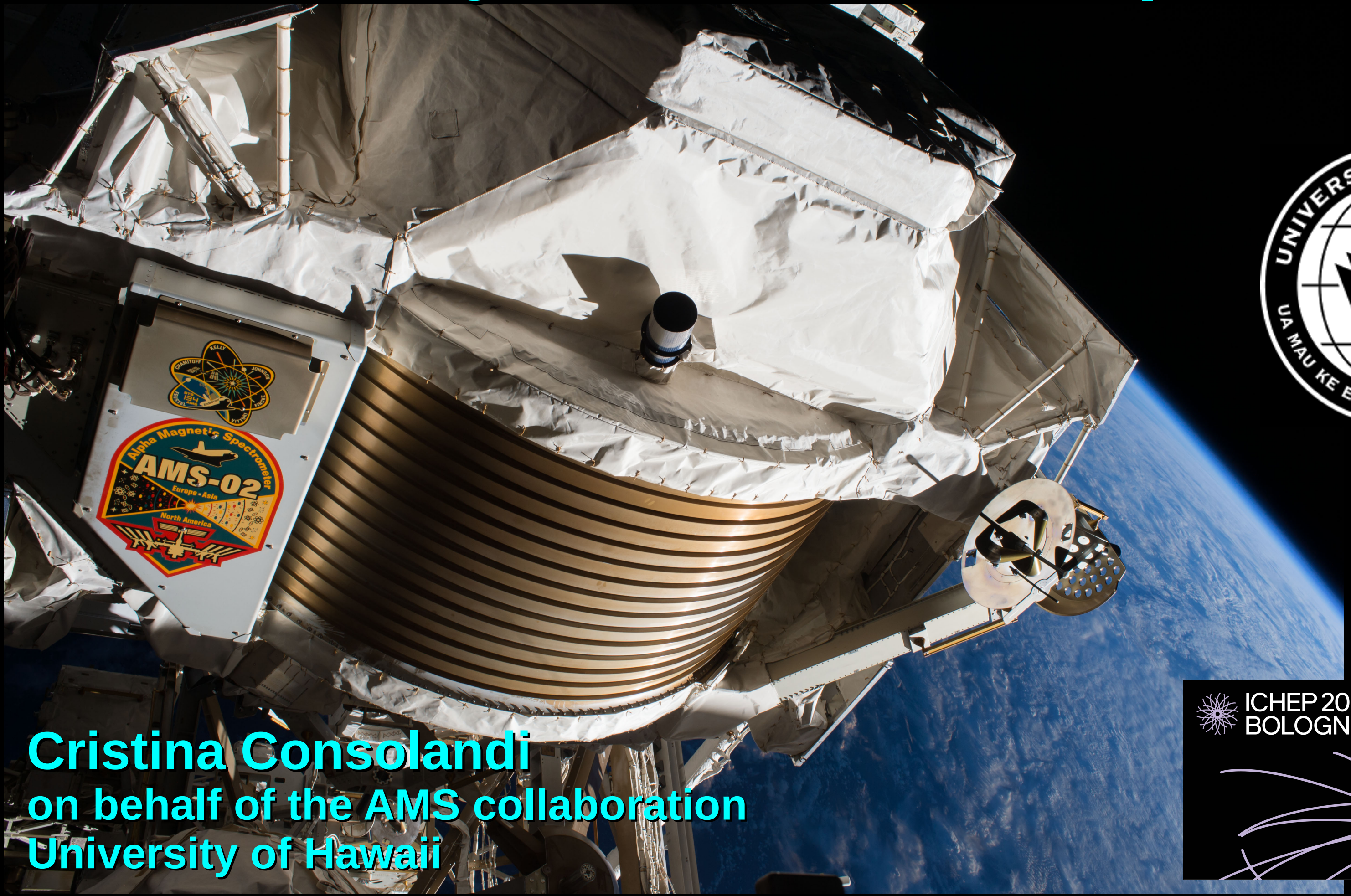

Cristina Consolandi
on behalf of the AMS collaboration
University of Hawaii

ICHEP 2022 BOLOGNA

ICHEP 2022
XLI
International Conference on High Energy Physics
Bologna (Italy)

Alpha Magnetic Spectrometer on ISS

AMS is a precision high energy particle detector on the International Space Station (ISS),
Near Earth Orbit ~400 km , inclination 52 deg, period 92 min.

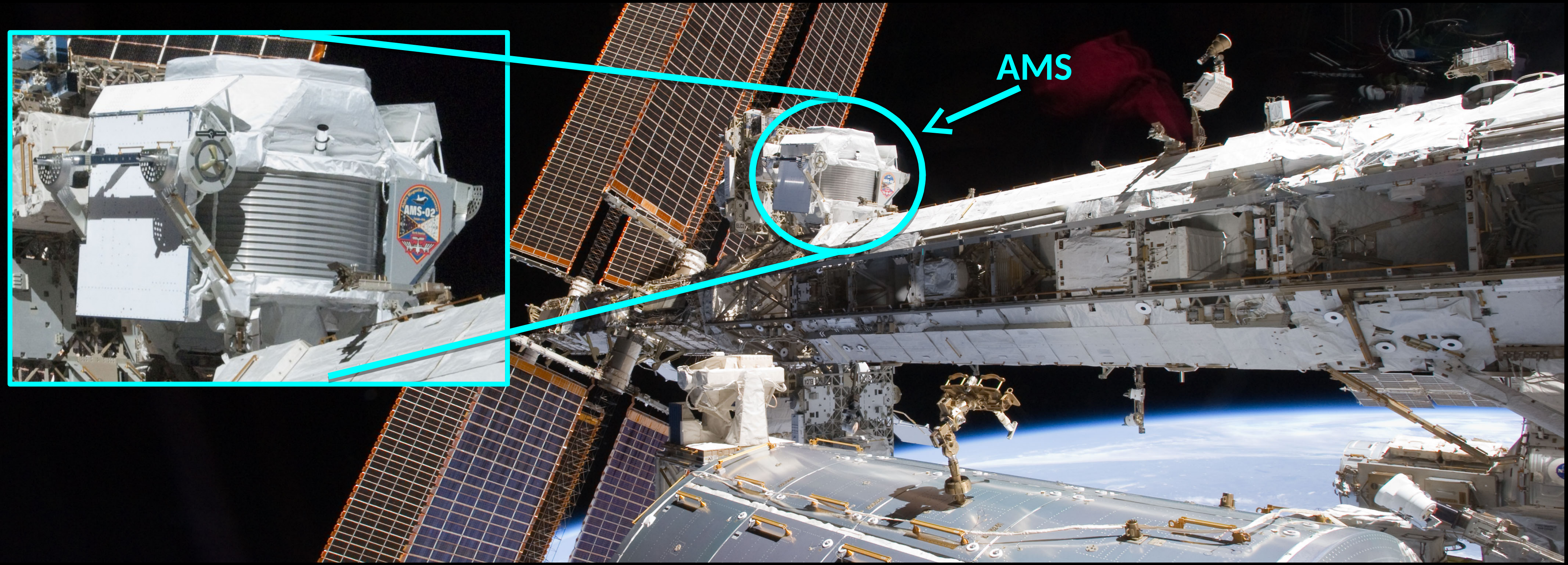

Since May 19th , 2011 AMS has collected over 205 billion
events and will continue through the lifetime of the ISS

Alpha Magnetic Spectrometer

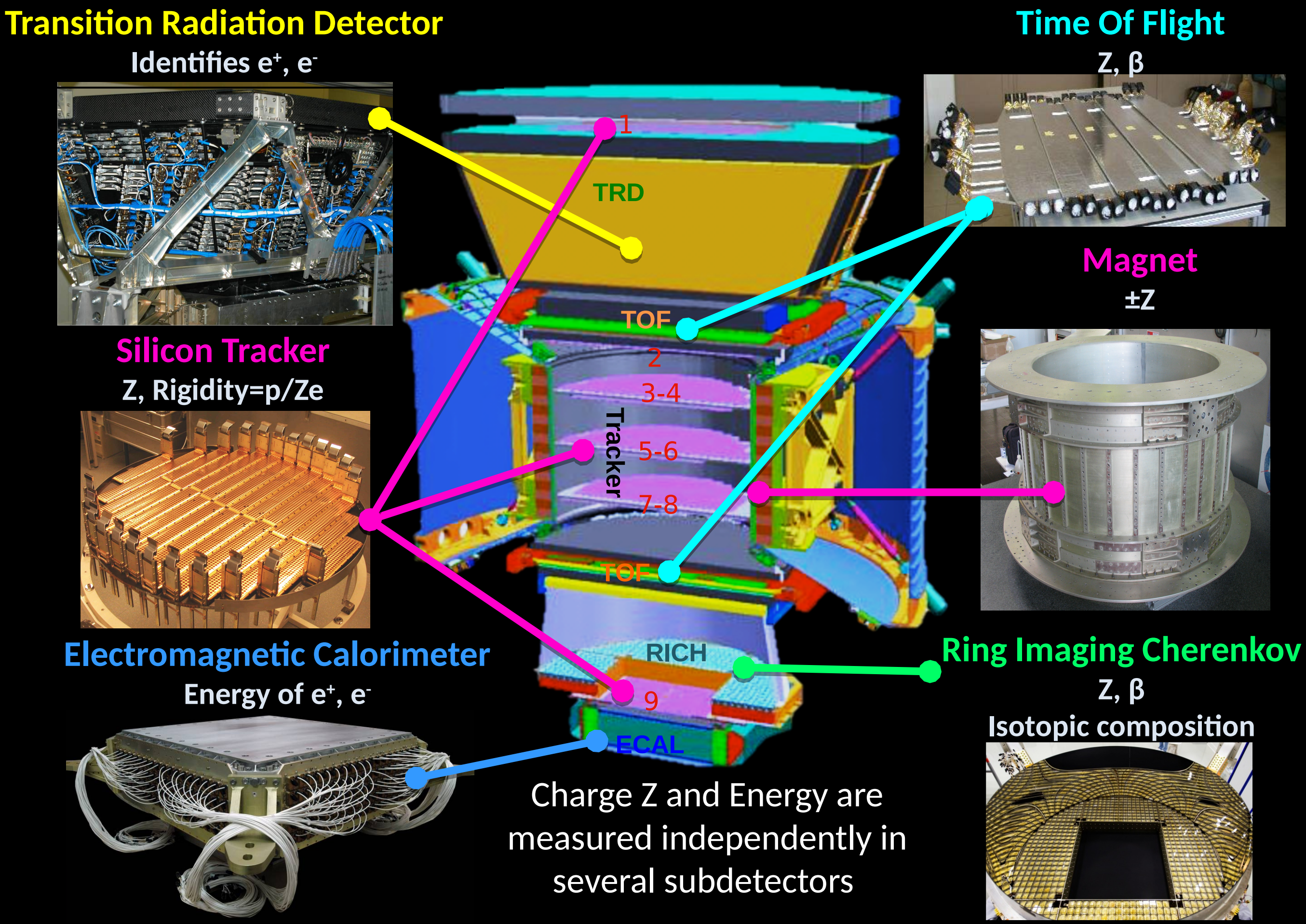

Charge Z and Energy are measured independently in several subdetectors

Solar Modulation of Low Energy Cosmic Rays

Cosmic rays entering the Heliosphere experience the influence of the solar activity.

The temporal evolution of the interplanetary space environment causes cosmic-ray intensity variations (i.e. solar modulation).

The solar modulation is particularly visible at rigidities below 100 GV, and it changes with the 11-years solar cycle.

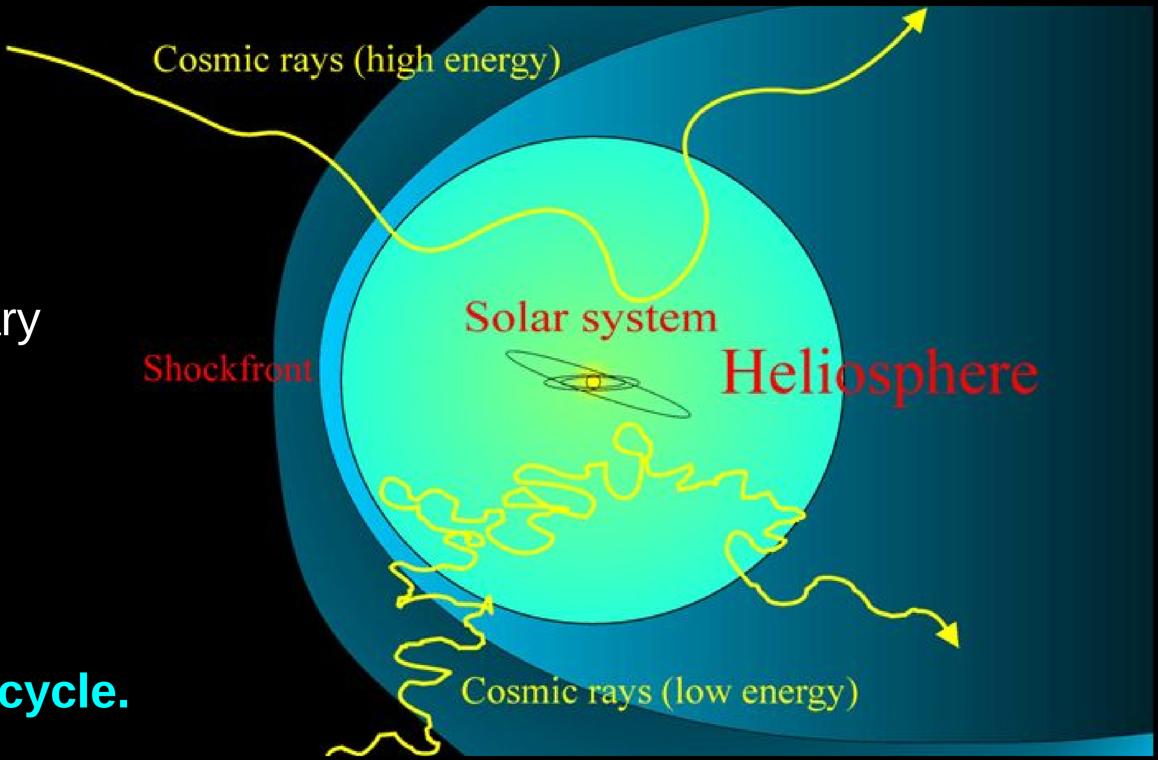

Daily Proton Fluxes: May 20, 2011 – May 2, 2021

6 billion protons collected from **May 20, 2011** to **May 2, 2021**

The proton flux exhibits variations on multiple timescales.

The relative magnitude of the variations decrease with increasing rigidity

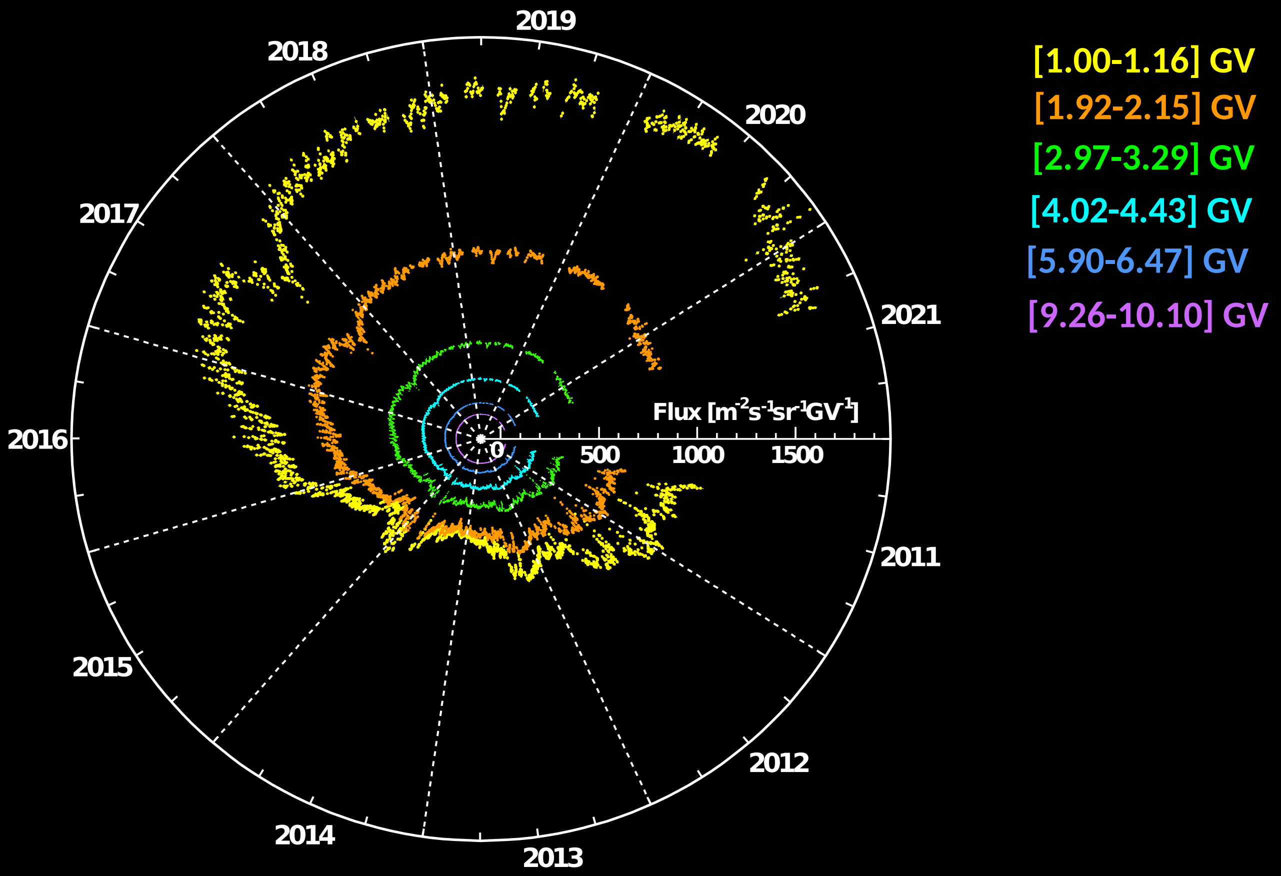

PRL 127, 272202 (2021)

AMS Daily Proton fluxes

The long scale variation is related to the 11-years Solar Cycle

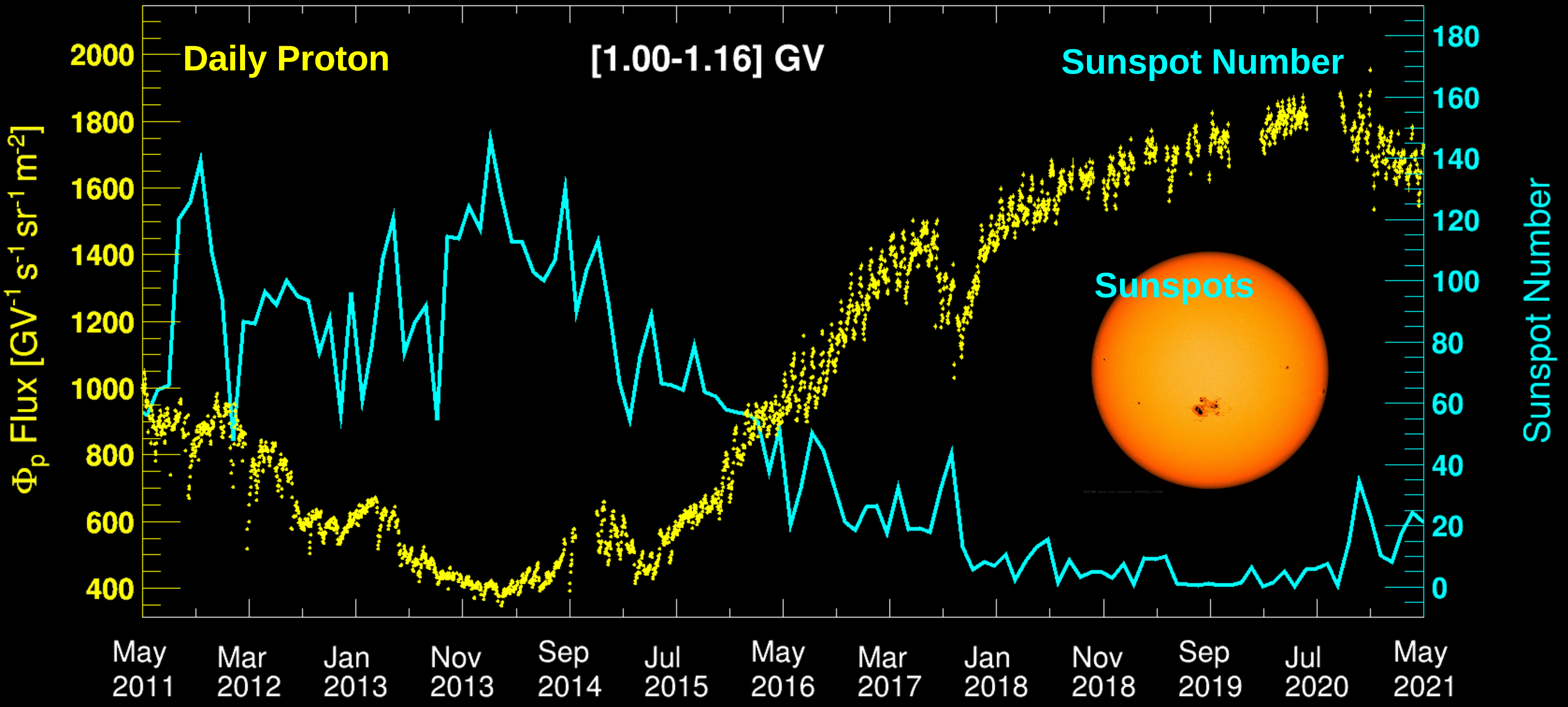

Sunspots are darker regions on the Sun with lower temperature and higher magnetic field

Daily Proton Fluxes: Nonrecurrent Variations

Short scale variations can be either **nonrecurrent** or **recurrent**

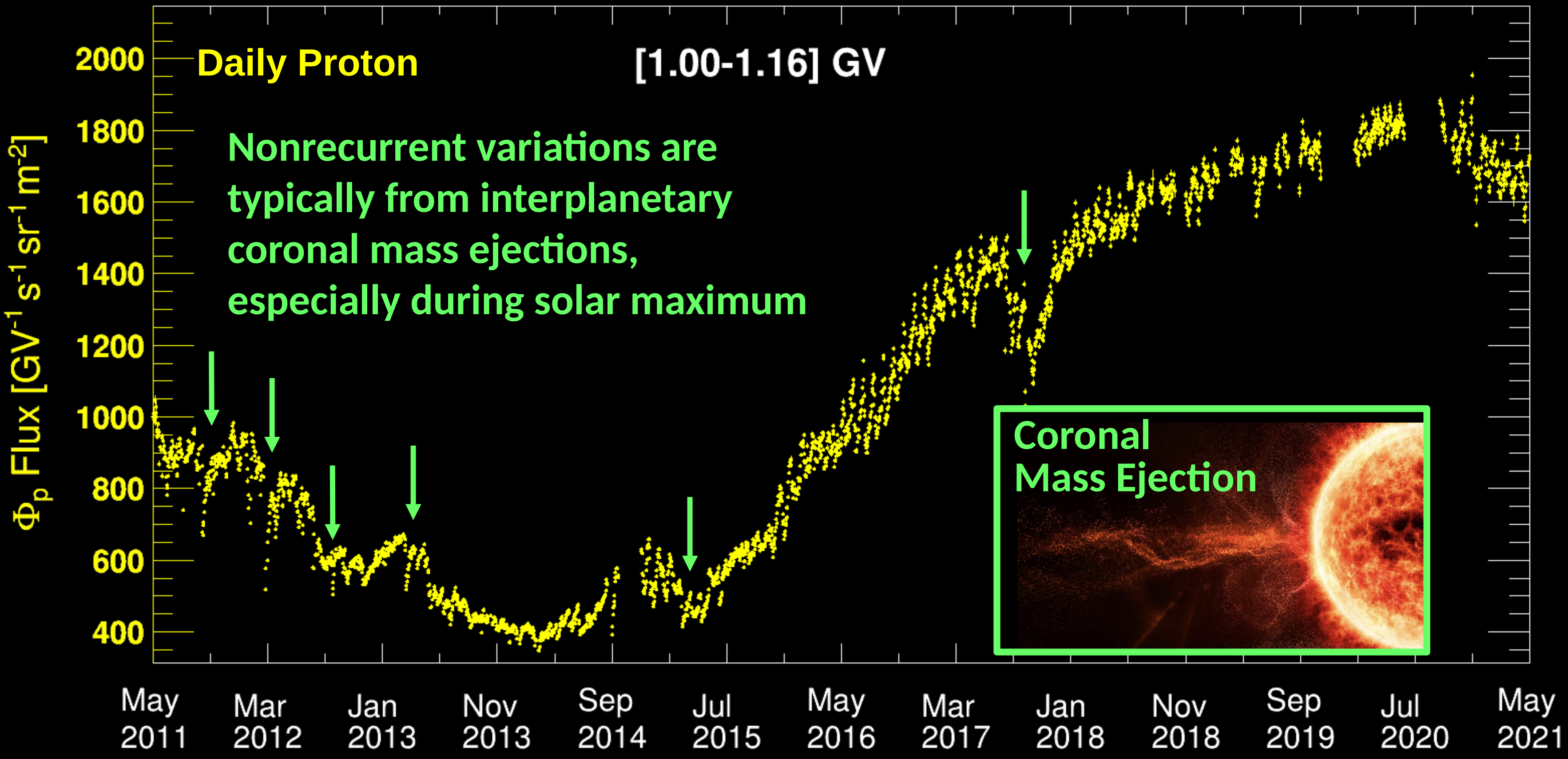

Daily Proton Fluxes: Recurrent Variations

Short scale variations can be either nonrecurrent or recurrent

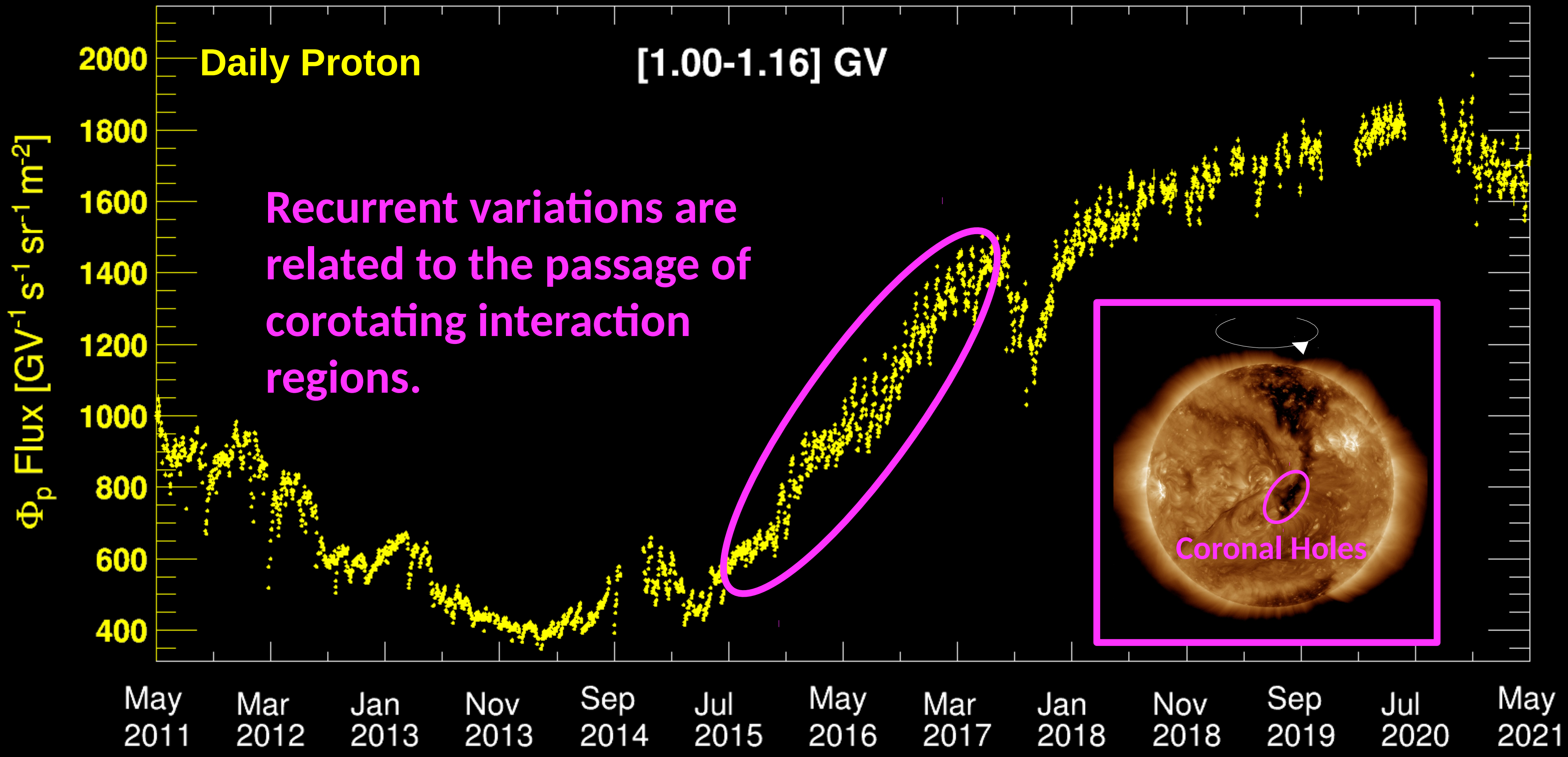

Sort Scale Recurrent Variations

Recurrent variations in cosmic rays are related to Sun's rotation (27 days, Bartels rotation).

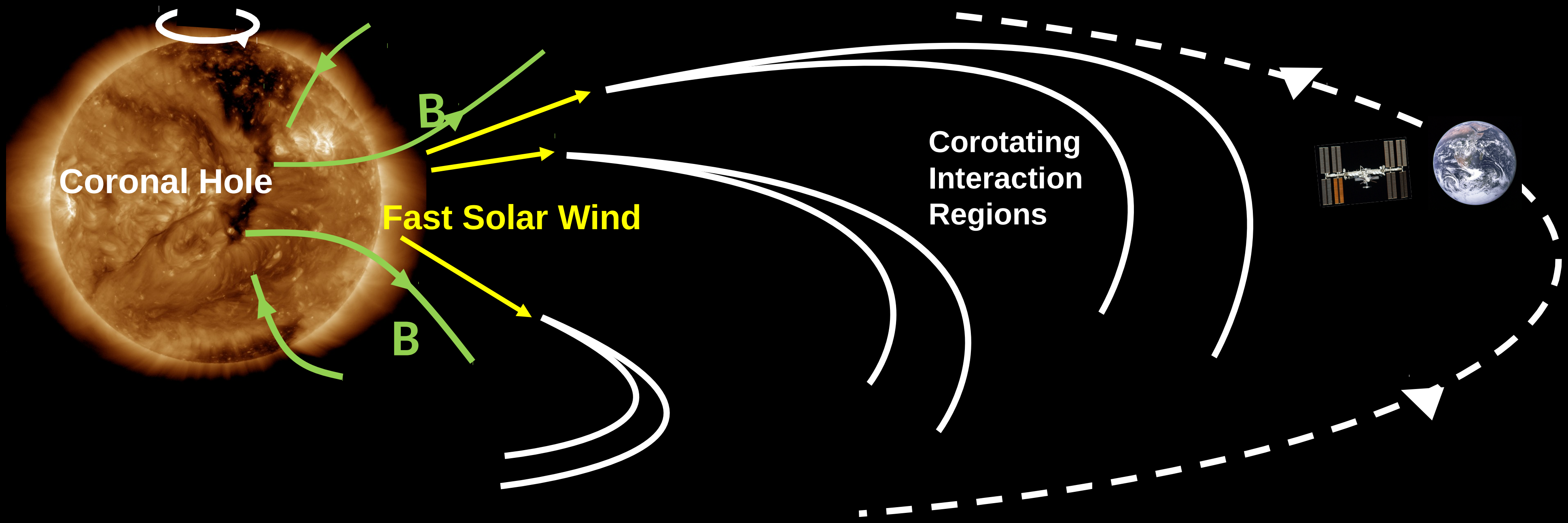

Coronal holes are regions where plasma density and temperature are lower, so they appear darker. Coronal Hole are **sources of fast solar wind** that interacting with the low solar wind creates **Corotating Interaction Regions** investing the Earth.

Recurrent Coronal Holes and Periodontics

Recurrent and multiple coronal hols head to multiple periodicity in the fluxes.

One coronal hole	→	27	days period
Two coronal holes separated by 180 deg	→	13.5	days period
Three coronal holes separated by 120 deg	→	9	days period

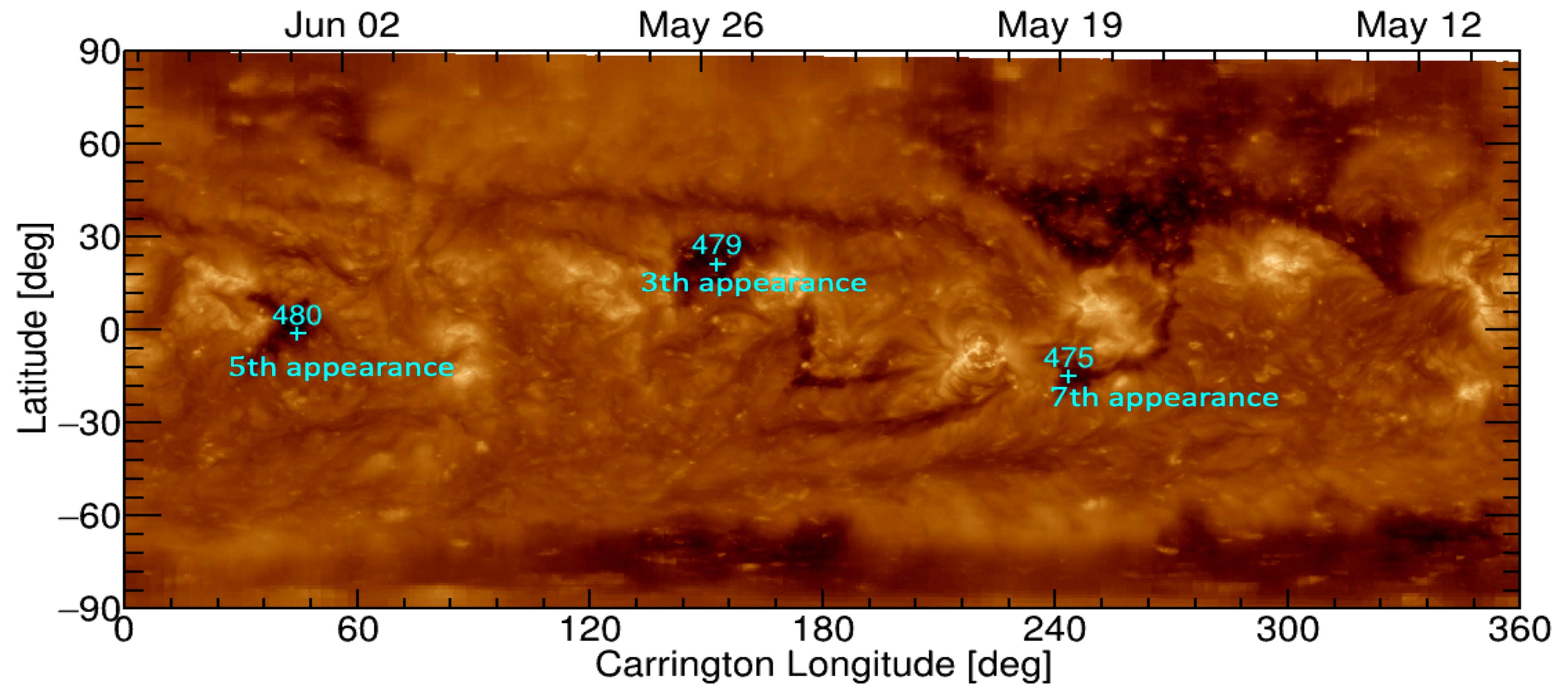

(May 10, 2016-Jun 06, 2016) Image taken by Solar Dynamics Observatory (SDO), NASA

Recurrent Daily Proton Flux Variations

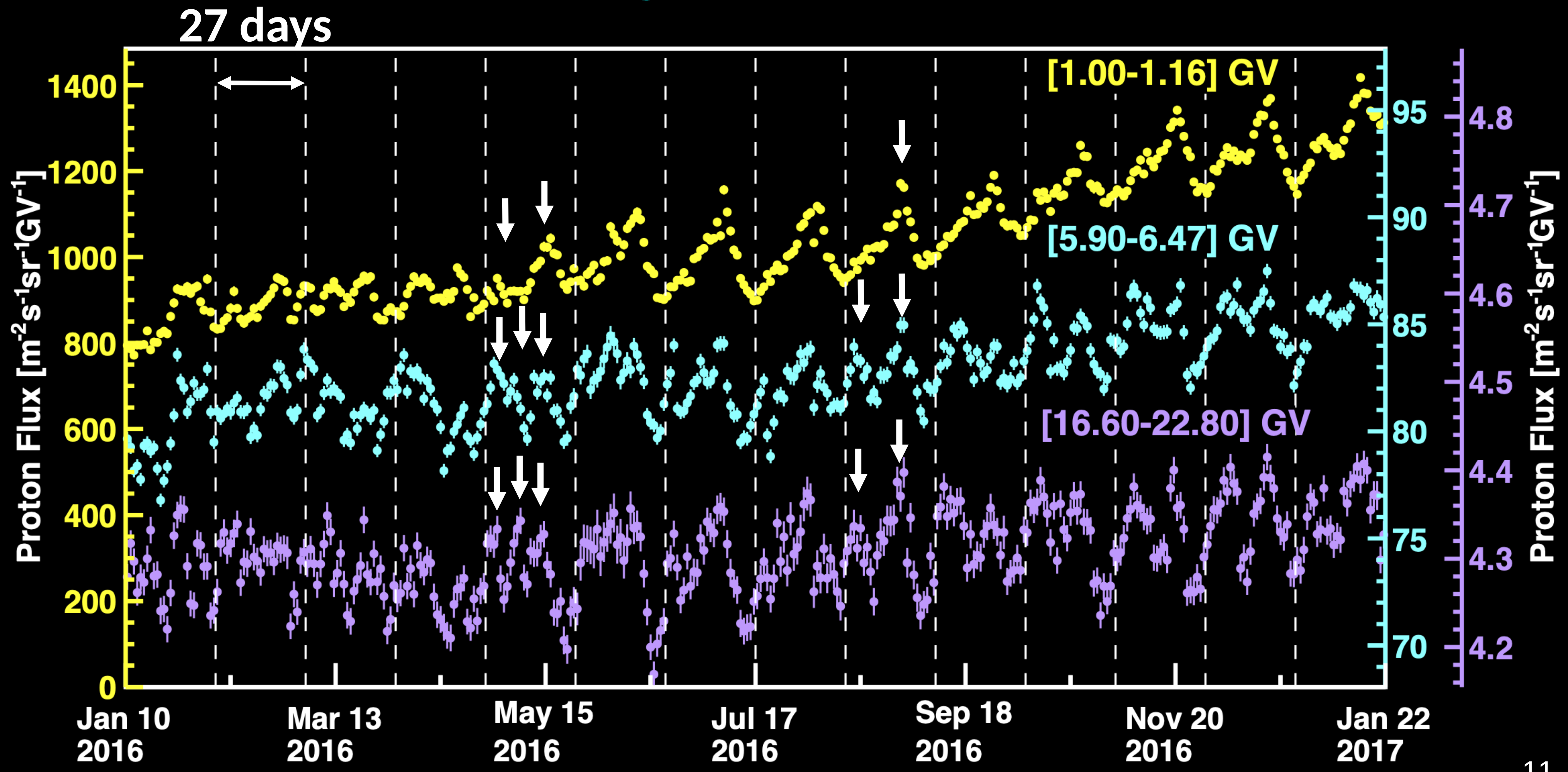

AMS daily Proton Flux and Solar Wind Speed

Anti-correlation exists with picks of flux in coincidence with valleys in the solar wind and vice versa.

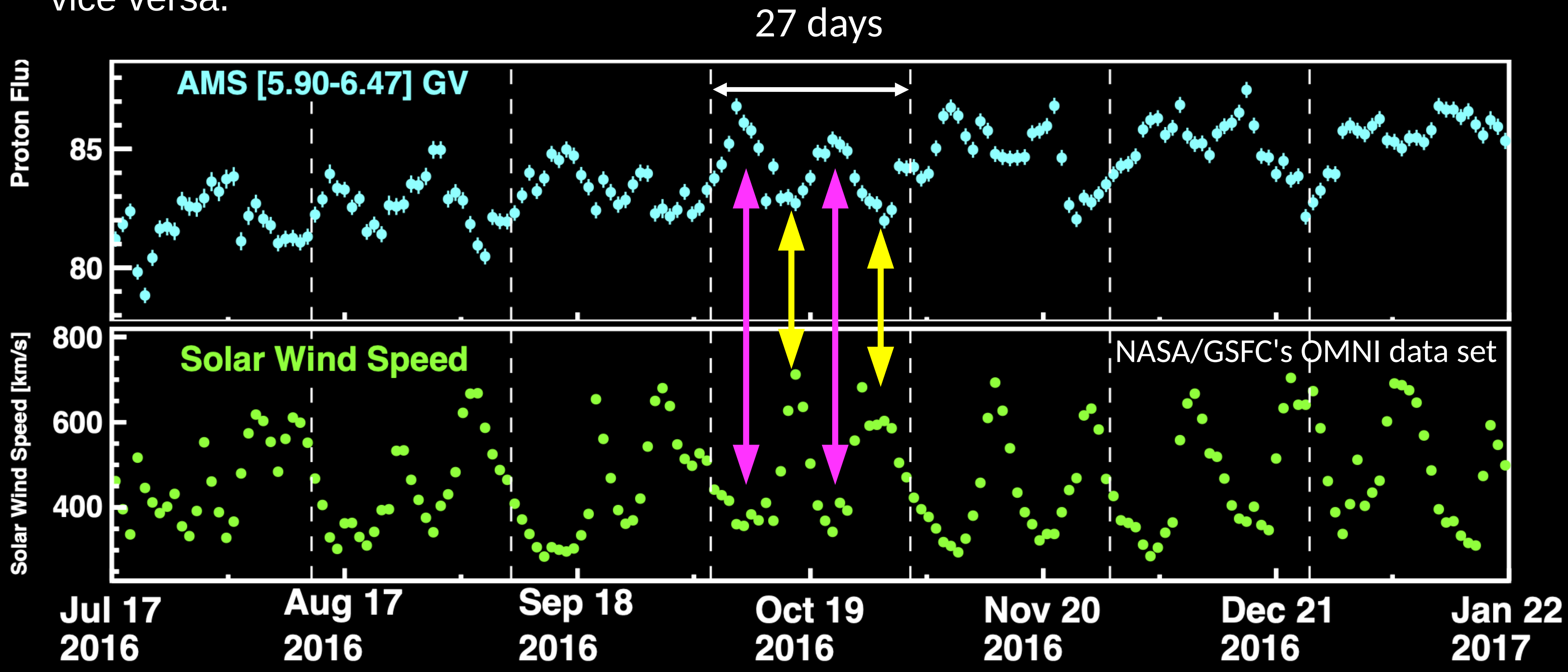

Wavelet Analysis on Proton Fluxes

To study the recurrent time variations, a **wavelet time-frequency technique was applied.**

The continuous wavelet transform W_n of a time series x_n with equal time interval δt is defined as:

$$|W_n(s)| = \sum_{n'=1}^{N} x_{n'} \psi^* [\frac{(n'-n)\delta t}{s}],$$

ψ is the wavelet function;
s is the period (1/frequency);
n is the day index.

$|W_n(s)|^2$ **is the power**

To show the **strength** of the periodicity, **the normalized power** is defined by the power divided by **the variance** of the time series.

C. Torrence and G. P. Compo, Bull. Am. Meteorol. Soc. 79, 61 (1998)

Daily AMS Proton Fluxes Measured in 2011-2012

2011 and 2012 do not have significant periods.

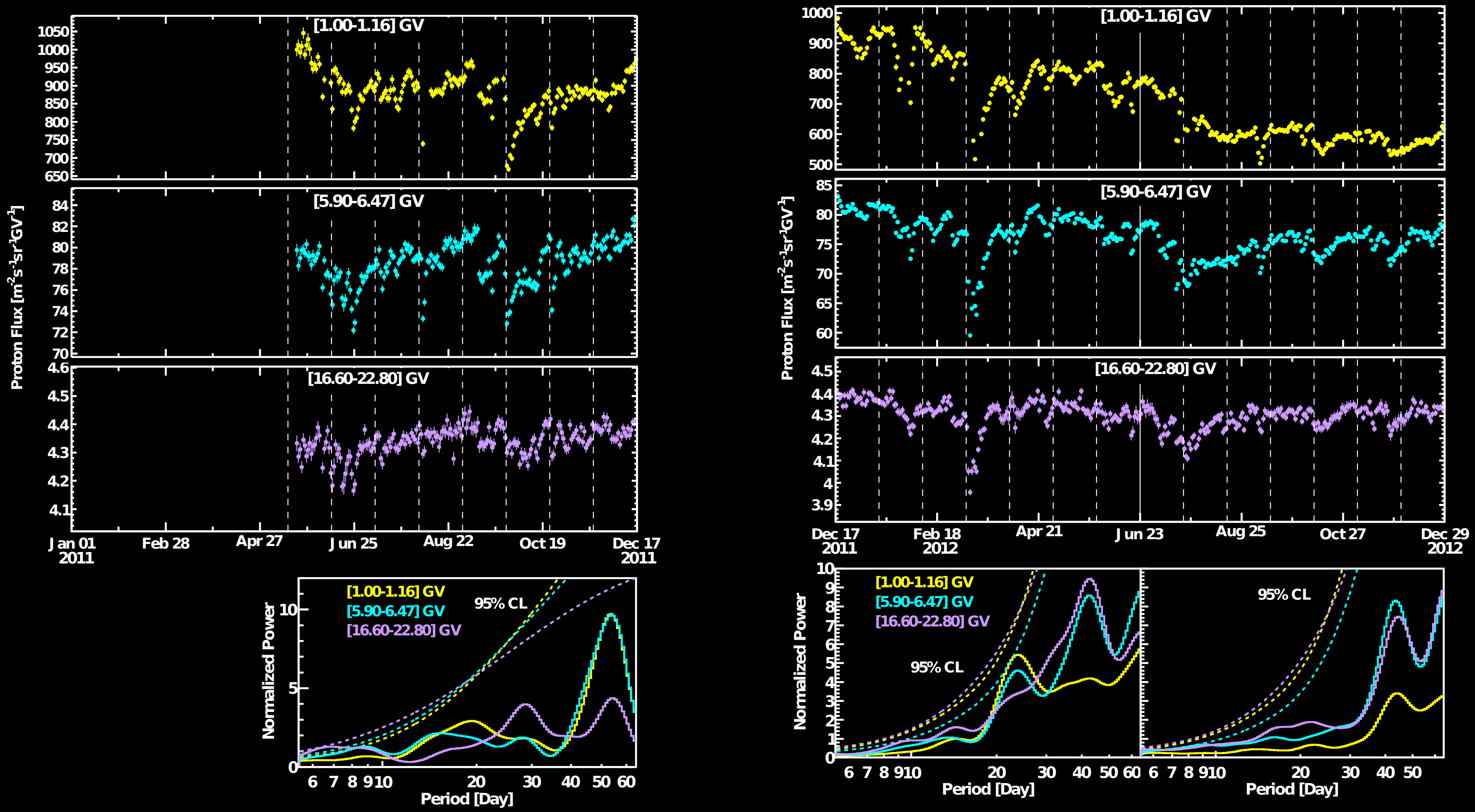

Daily AMS Proton Fluxes Measured in 2013-2014

2013 does not have significant periods.

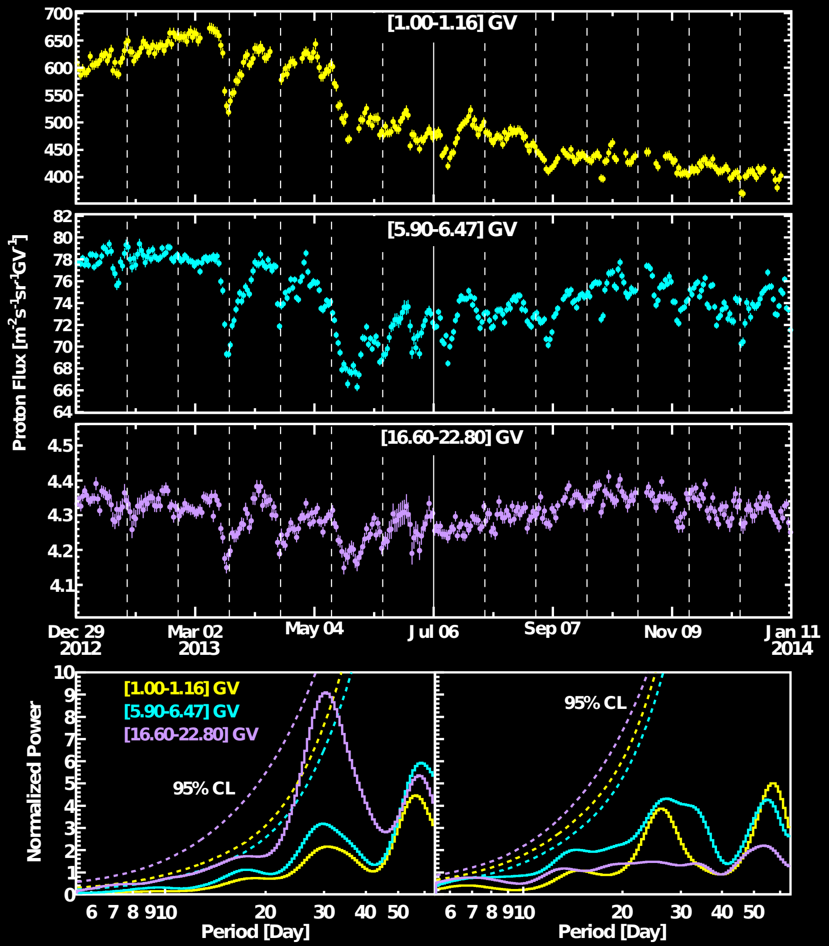

27-days period in observed in 2014

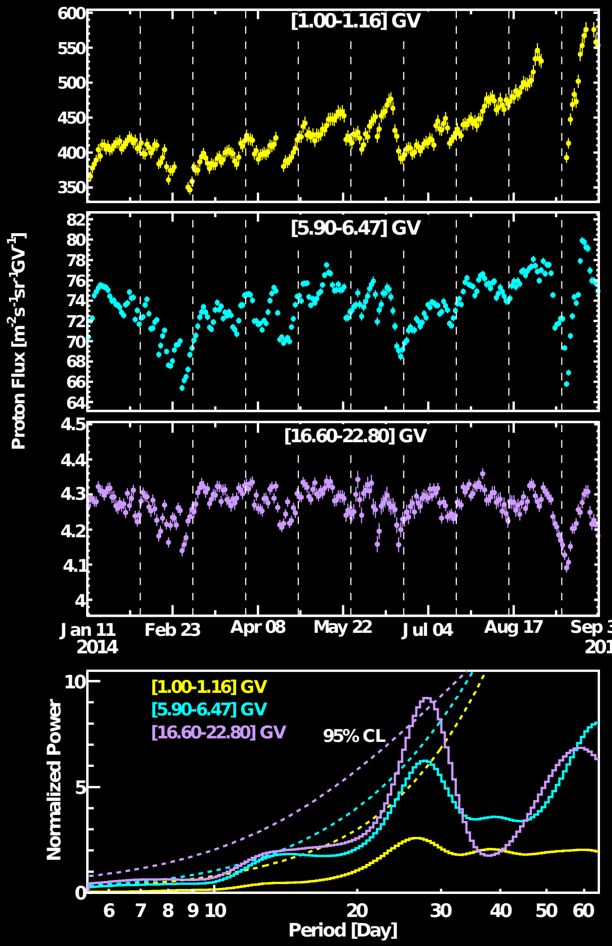

Daily AMS Proton Fluxes Measured in 2015-2016

27-days period is observed in 2015

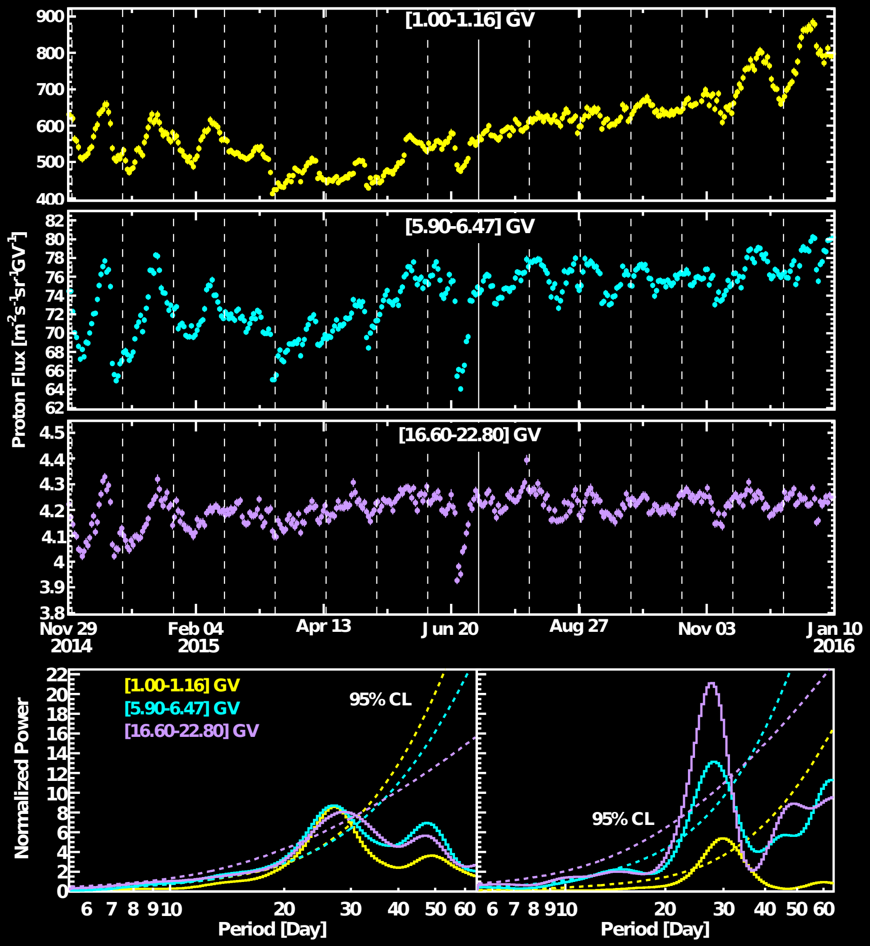

27, 13.5, 9 days periods are observed in 2016

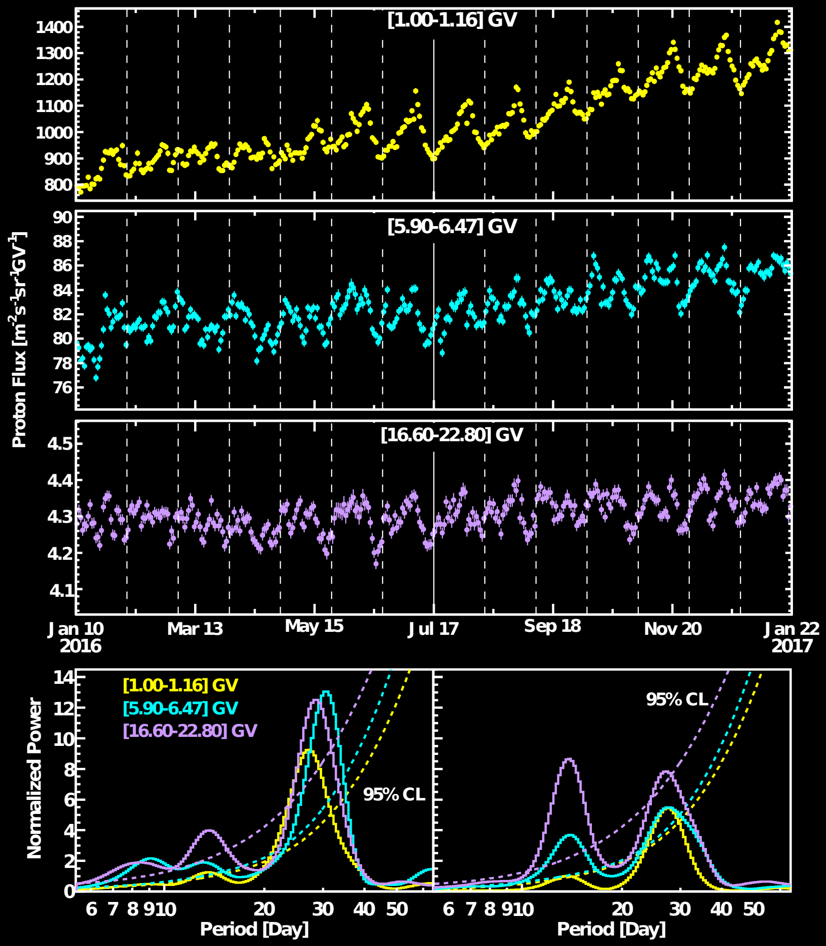

Daily AMS Proton Fluxes Measured in 2017-2018

27-days period is observed in 2017and 2018

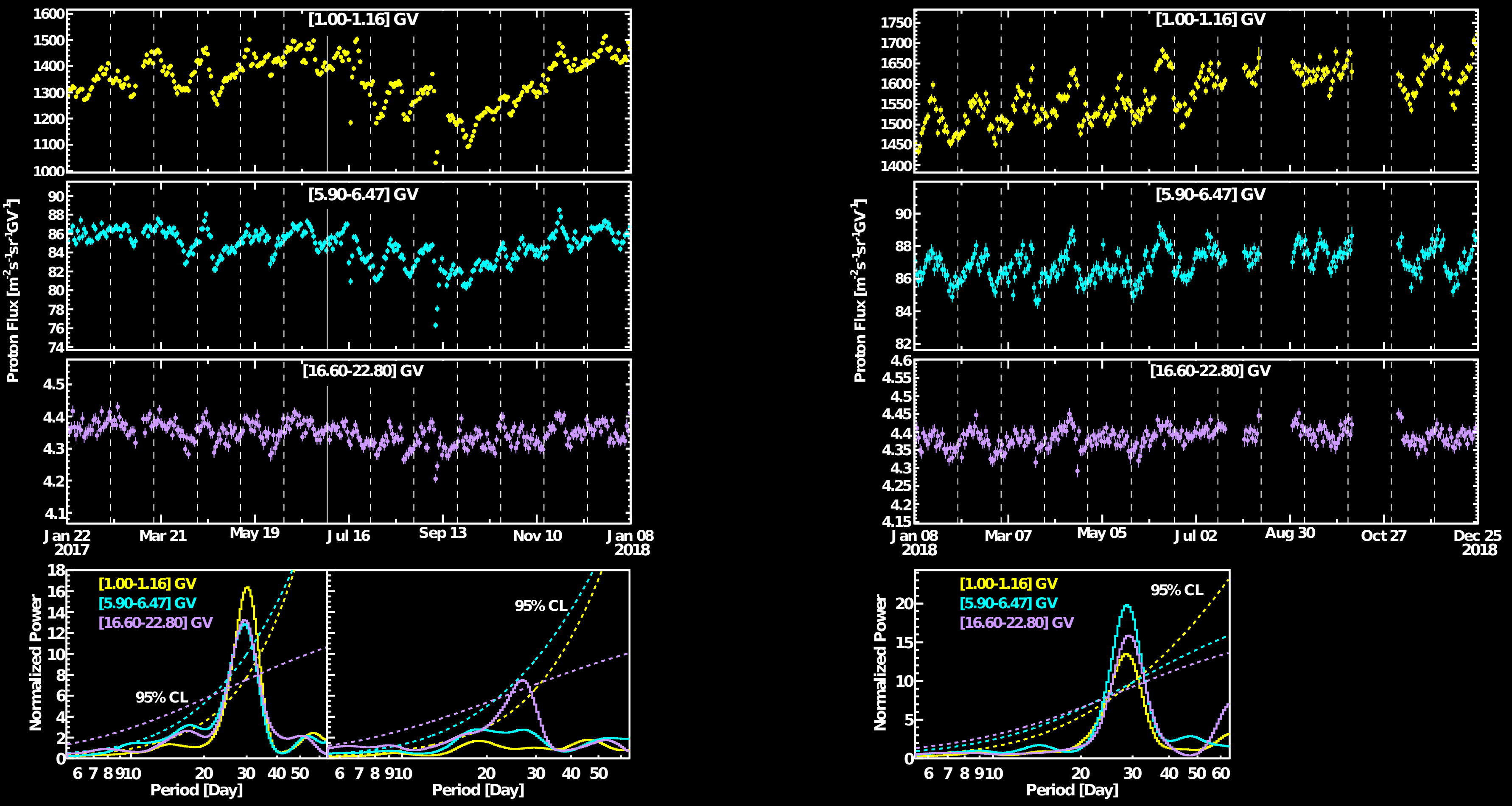

The wavelet Analysis of Proton fluxes in 2016

To show the strength of the periodicity, **the normalized power** is defined by the **power divided by the variance** of the time series.

Periods of 9, 13.5, and 27 days are observed in 2016.

The strength of all three periodicities change with time and rigidity.

In particular, shorter periods of 9 and 13.5 days, when present, are more visible at 6 GV and 20 GV compared to 1 GV.

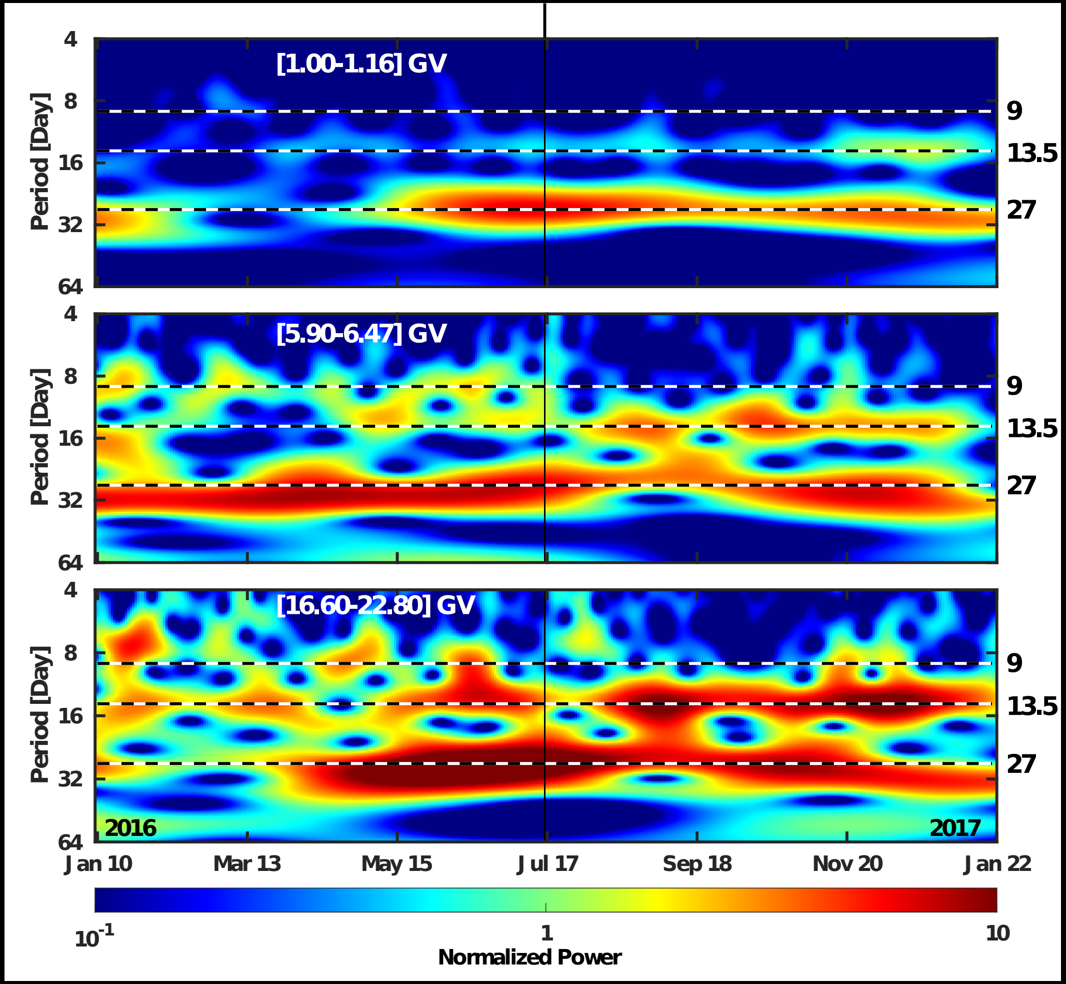

Power spectra of Proton Fluxes averaged over the First and Second Half of 2016

In the first half of 2016:
the strengths of **9-day and 13.5-day periods** increase with increasing rigidity.

In the second half of 2016:
the strength of **the 13.5-day period** increases with increasing rigidity, and **the 9-day period** is not visible.

The strength of **the 27-day period** varies with rigidity in both time intervals.

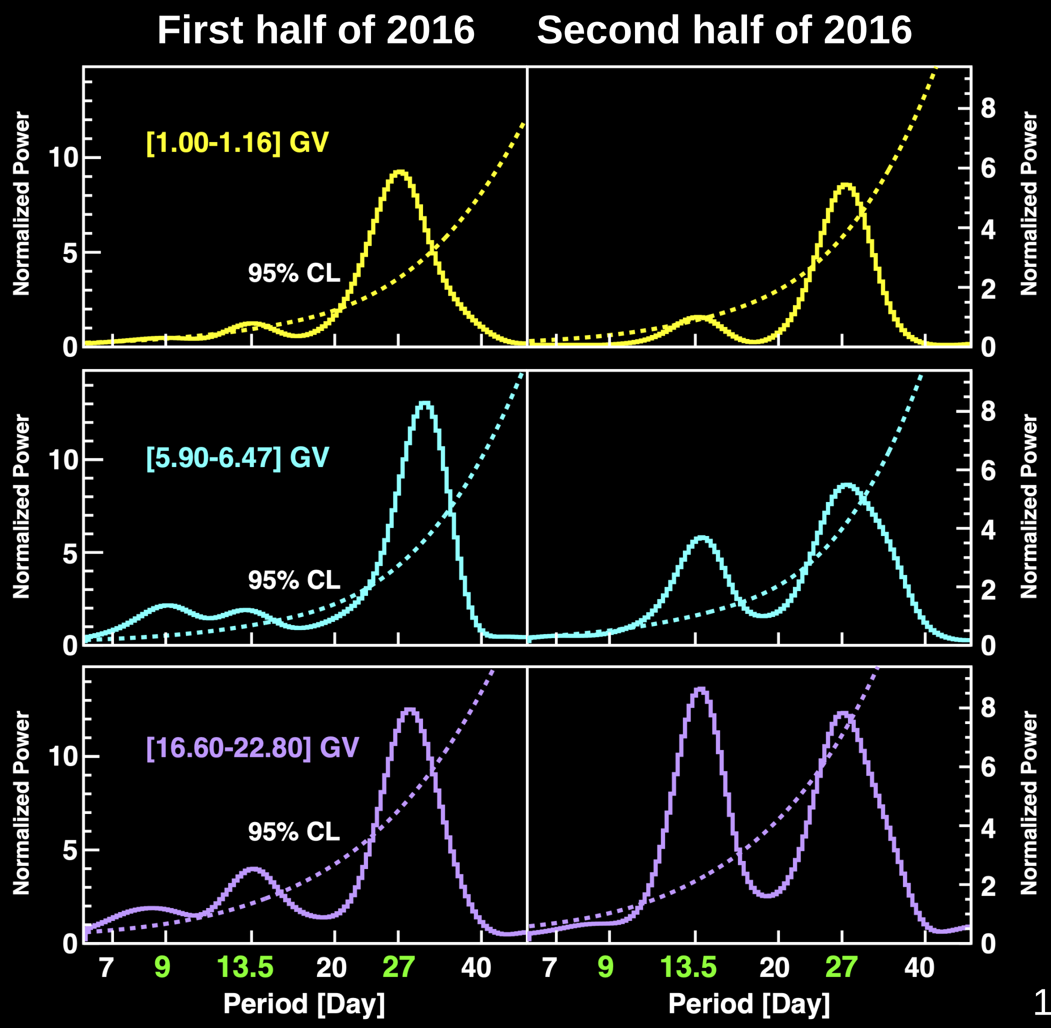

Periodicity of daily Proton Fluxes in 2016

Unexpectedly, the strength of **9-day and 13.5-day periodicities** increases with increasing rigidity up to **10 GV** and **20 G,** respectively. Then the strength decreases with increasing rigidity up to **100 GV.**

Thus, the AMS results do not support the general conclusion that the strength of the periodicities always decreases with increasing rigidity

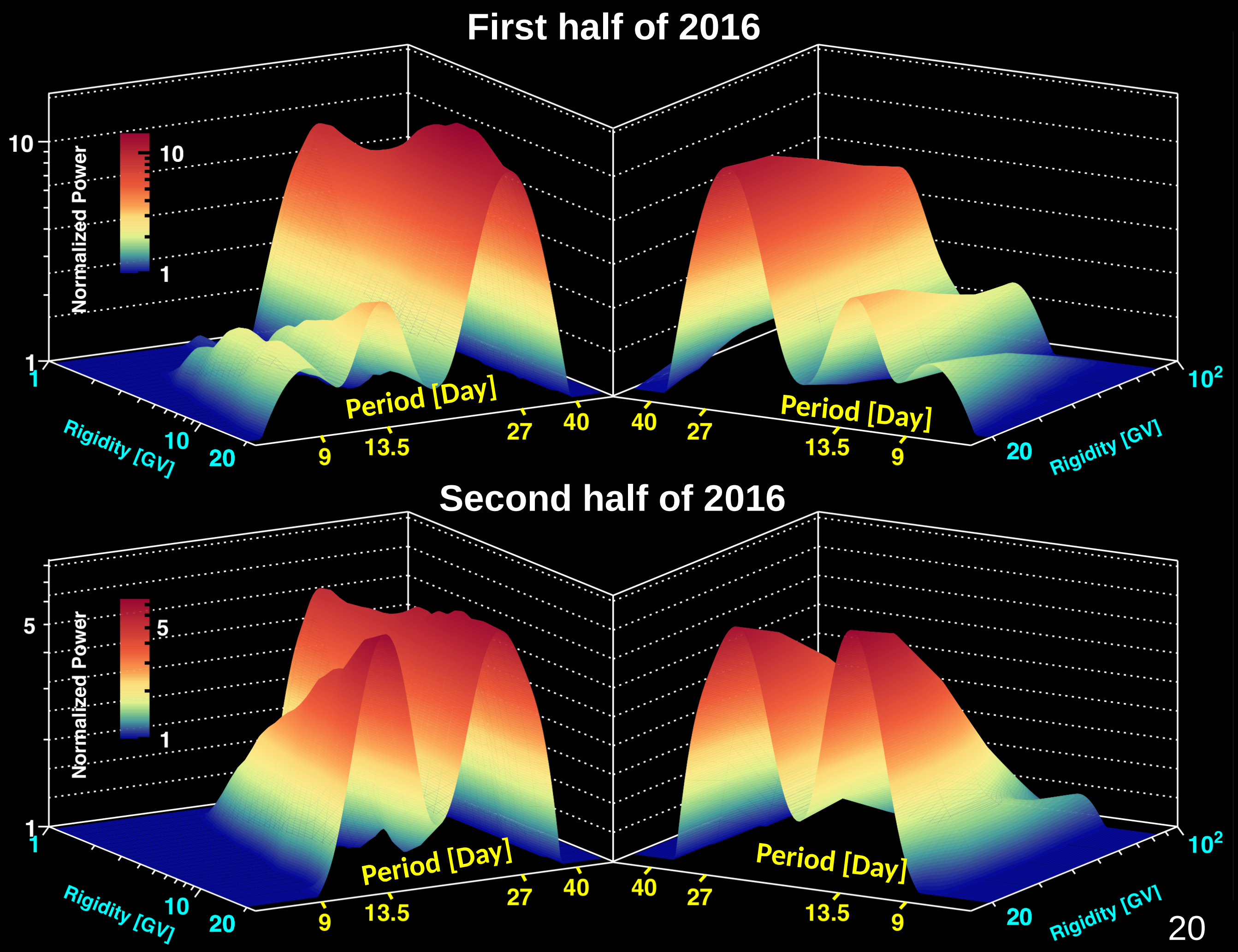

Summary

- We have presented the precision measurements of the daily proton fluxes in cosmic rays **from 1 GV to 100 GV** between **May 20, 2011 and May 2, 2021** based on 6 billion protons. The proton fluxes exhibit variations on multiple time scales.

- From **2014 to 2018**, we observed recurrent flux variations with a period of **27 days**. Shorter periods of **9 days and 13.5 days** are observed in 2016.

- The strength of all three periodicities changes with both time and rigidity. Unexpectedly, the strength of **9-day and 13.5-day** periodicities increases with increasing rigidities up to **10 GV and 20 GV** respectively. Then the strength decreases with increasing rigidity up to **100 GV**. **The AMS results do not support the general conclusion that the strength of the periodicities always decreases with increasing rigidity.**

Future Measurements of Daily Proton Flux

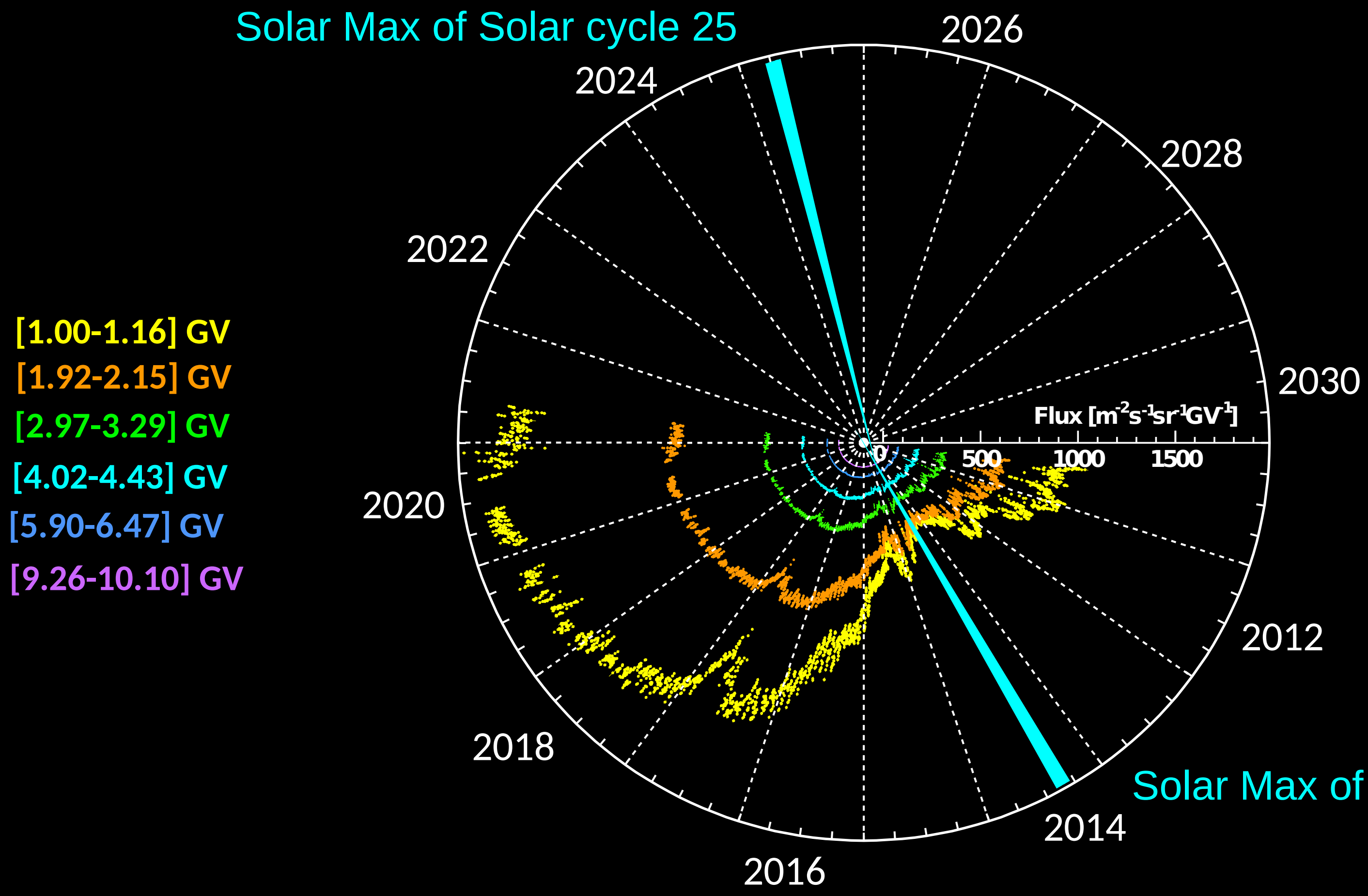

AMS will continue through the lifetime of the ISS

AMS observations provide inputs to the understanding of cosmic ray propagation in the heliosphere.

Backup

Wavelet Analysis on Proton Fluxes

Continuous Wavelet Transform:

$$W_n(s) = \sum_{n'=1}^{N} x_{n'} \psi^* \left[\frac{(n' - n)\delta t}{s} \right]$$

Morlet wavelet, ie. plane wave modulated by a Gaussian:

$$\psi(\eta) = \pi^{-1/4} e^{i6\eta} e^{-\eta^2/2}$$

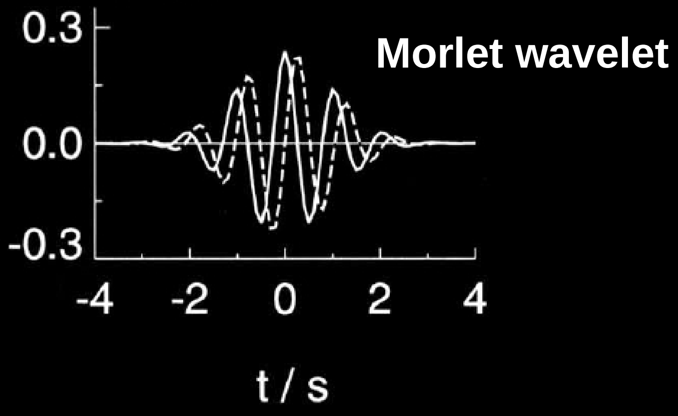

Variance of the time series:

$$\sigma^2 = \frac{\sum_{n=n_1}^{n_2} (x_n - \overline{x})^2}{n_2 - n_1}$$

C. Torrence and G. P. Compo, Bull. Am. Meteorol. Soc. 79, 61 (1998)

95% Confidence Level

Monte Carlo simulation are used to asses the statistical significance against backgrounds which are generated by the lag-1 autoregressive process:

$$y_n = \alpha y_{n-1} + z_n$$

z_n is a Gaussian with zero mean and width such that the variance of the simulated time series is equal to the measured time series. Lag-1 autocorrelation is obtained from the measured time series x_n:

$$\alpha = \frac{\sum_{n=1}^{N-1}(x_n - \overline{x})(x_{n+1} - \overline{x})}{\sum_{n=1}^{N}(x_n - \overline{x})^2}$$

95% CL is obtained by the power exceeded by 5% of the power values calculated from the simulated background.

C. Torrence and G. P. Compo, Bull. Am. Meteorol. Soc. 79, 61 (1998)

Daily He, p and He/p Flux Ratio

The helium to proton flux ratio exhibits variations on multiple timescales.

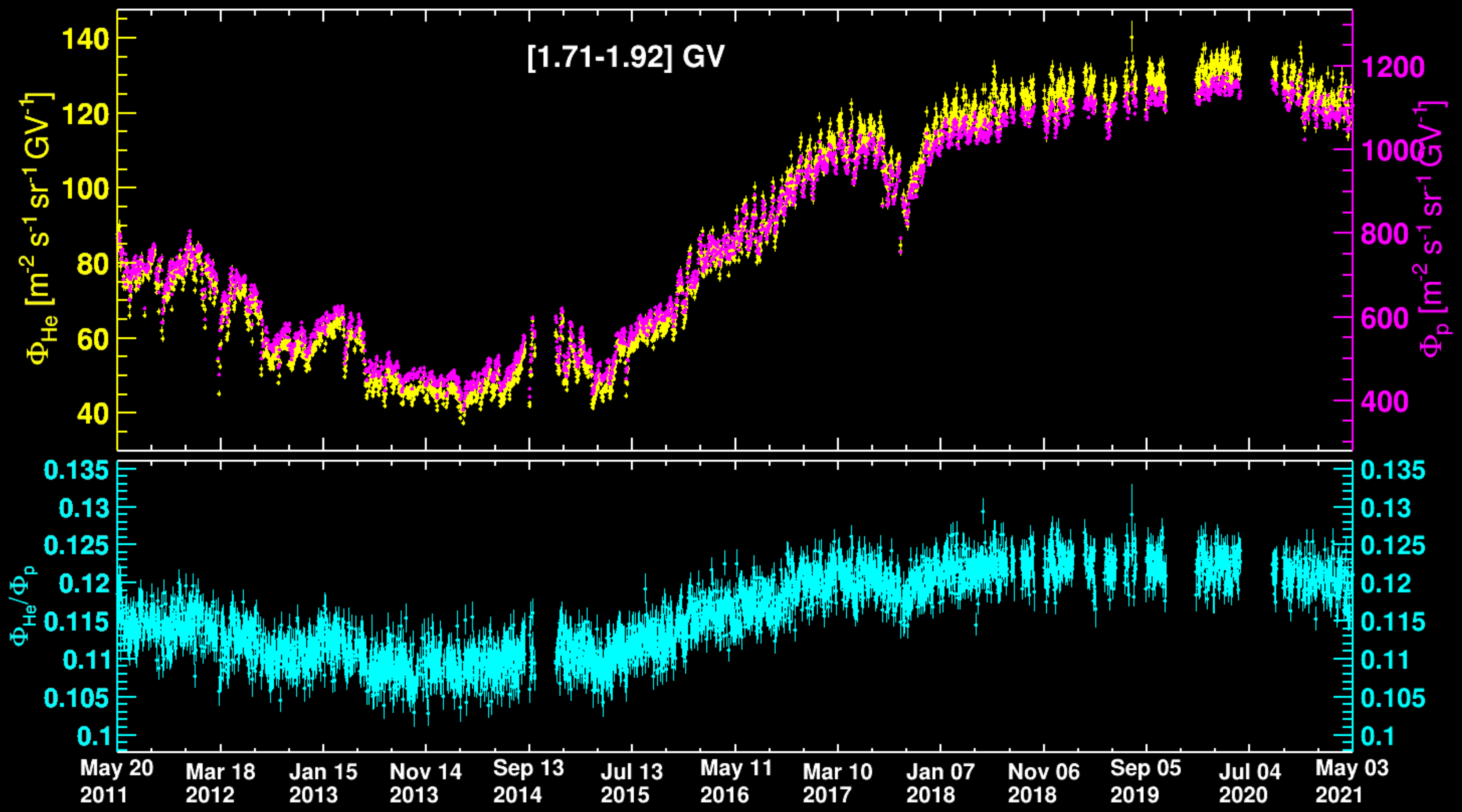

Daily He, p and He/p Flux Ratio

The helium flux exhibits larger time variations than the proton flux

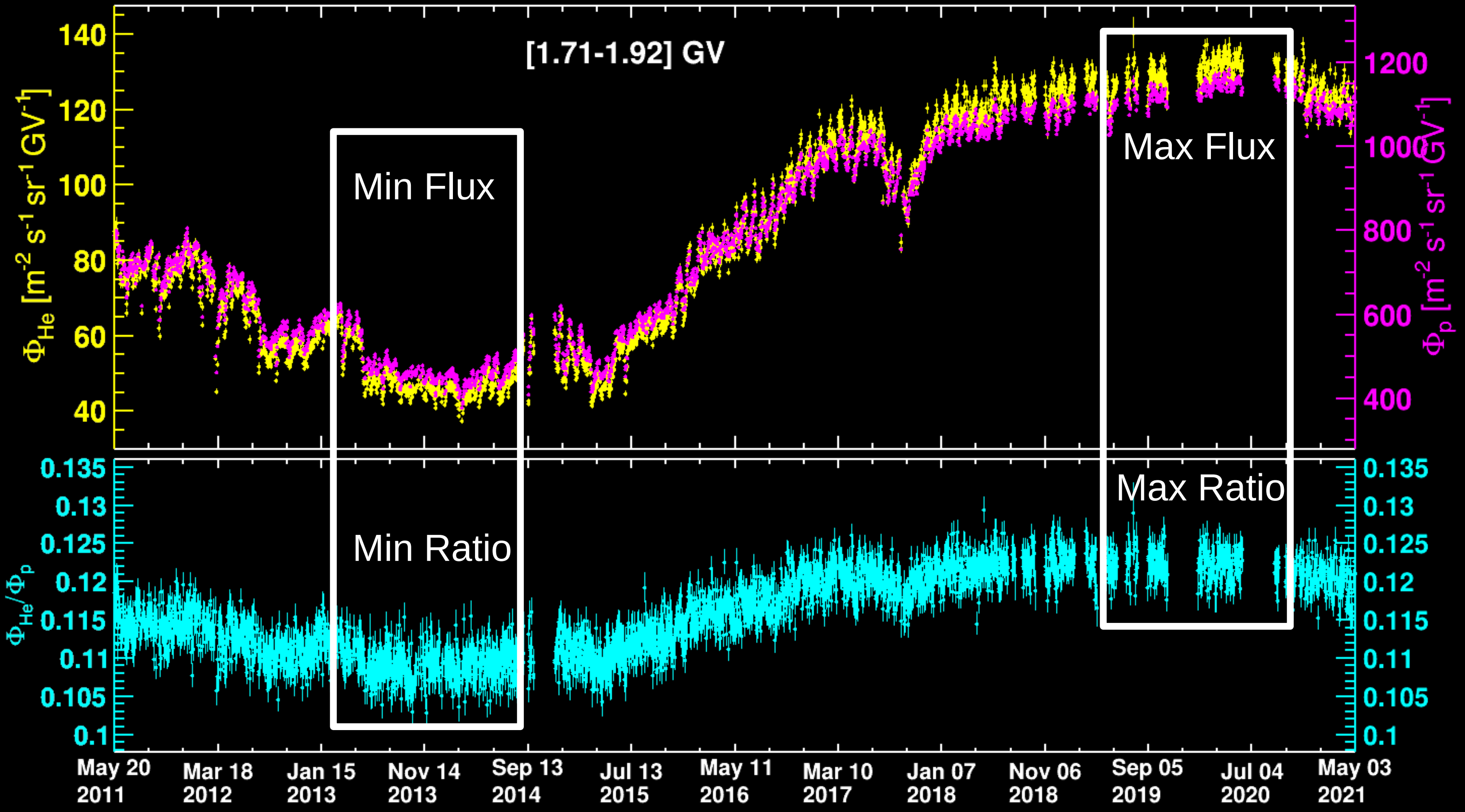

Daily He, p and He/p Flux Ratio

Above ~ 7 GV the helium to proton flux ratio is time-independent

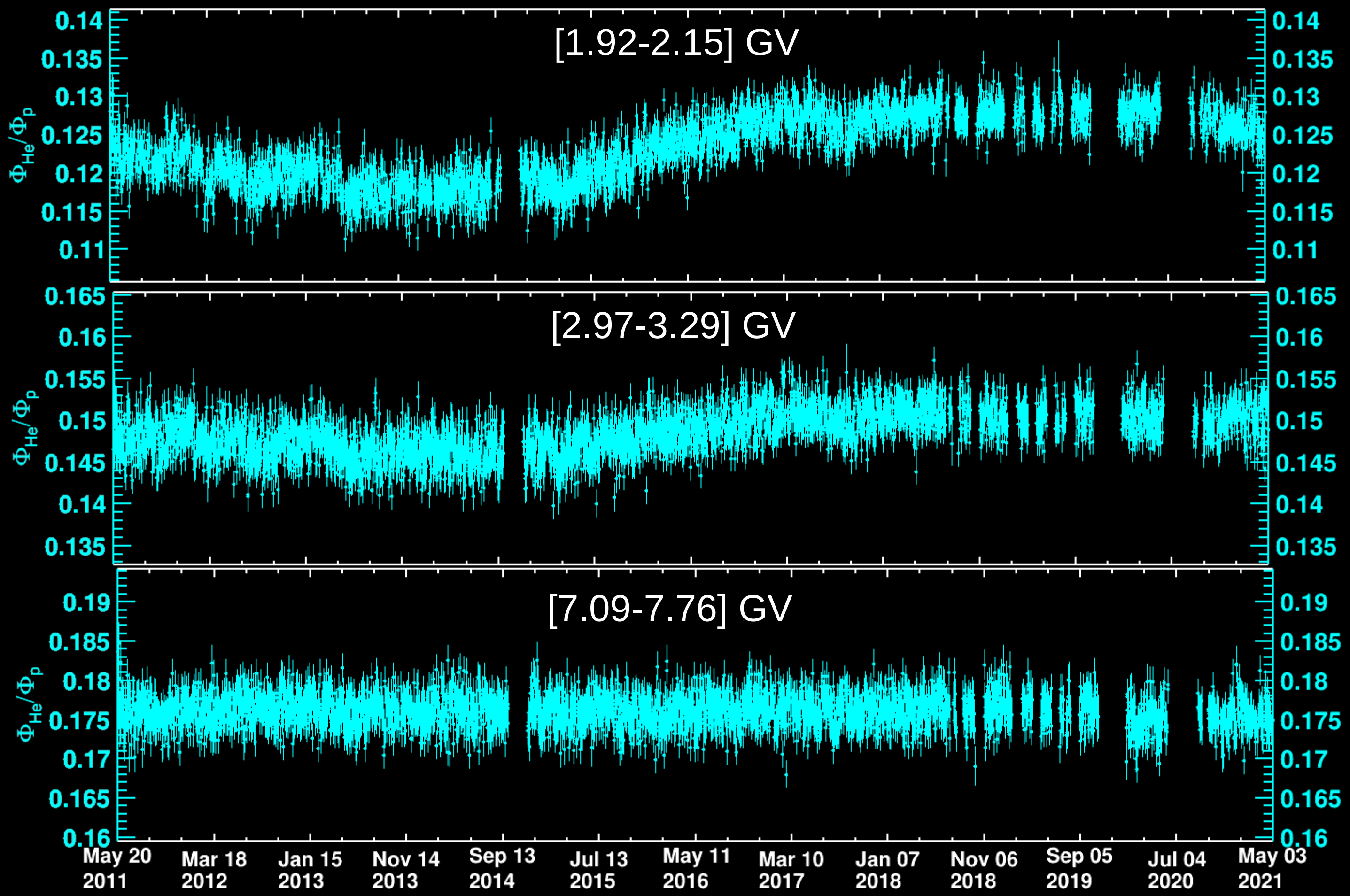

Daily He/p Flux Ratio vs. He Flux

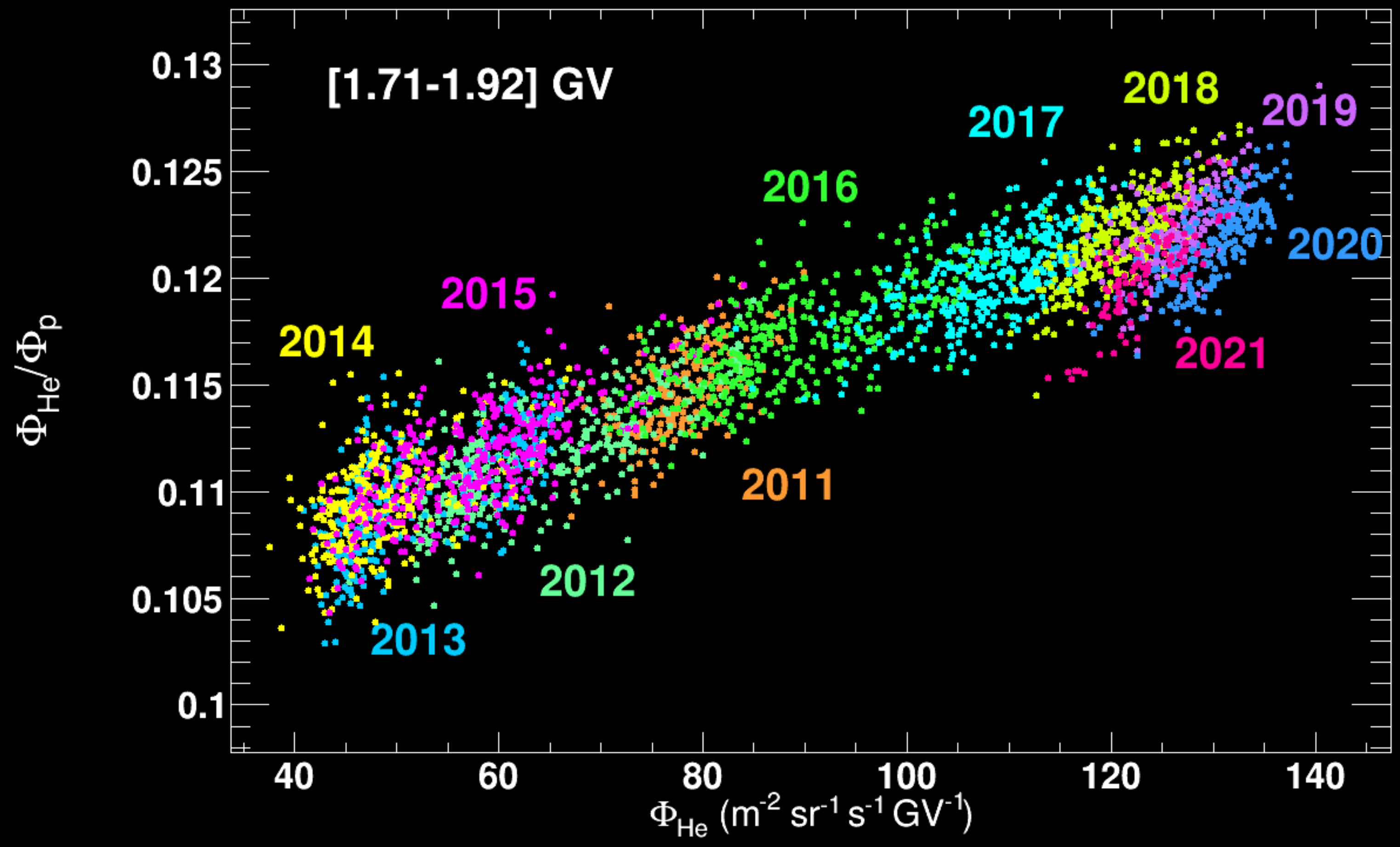

Hysteresis between He/p Flux Ratio and He Flux

▲ Before solar maximum
■ After solar maximum

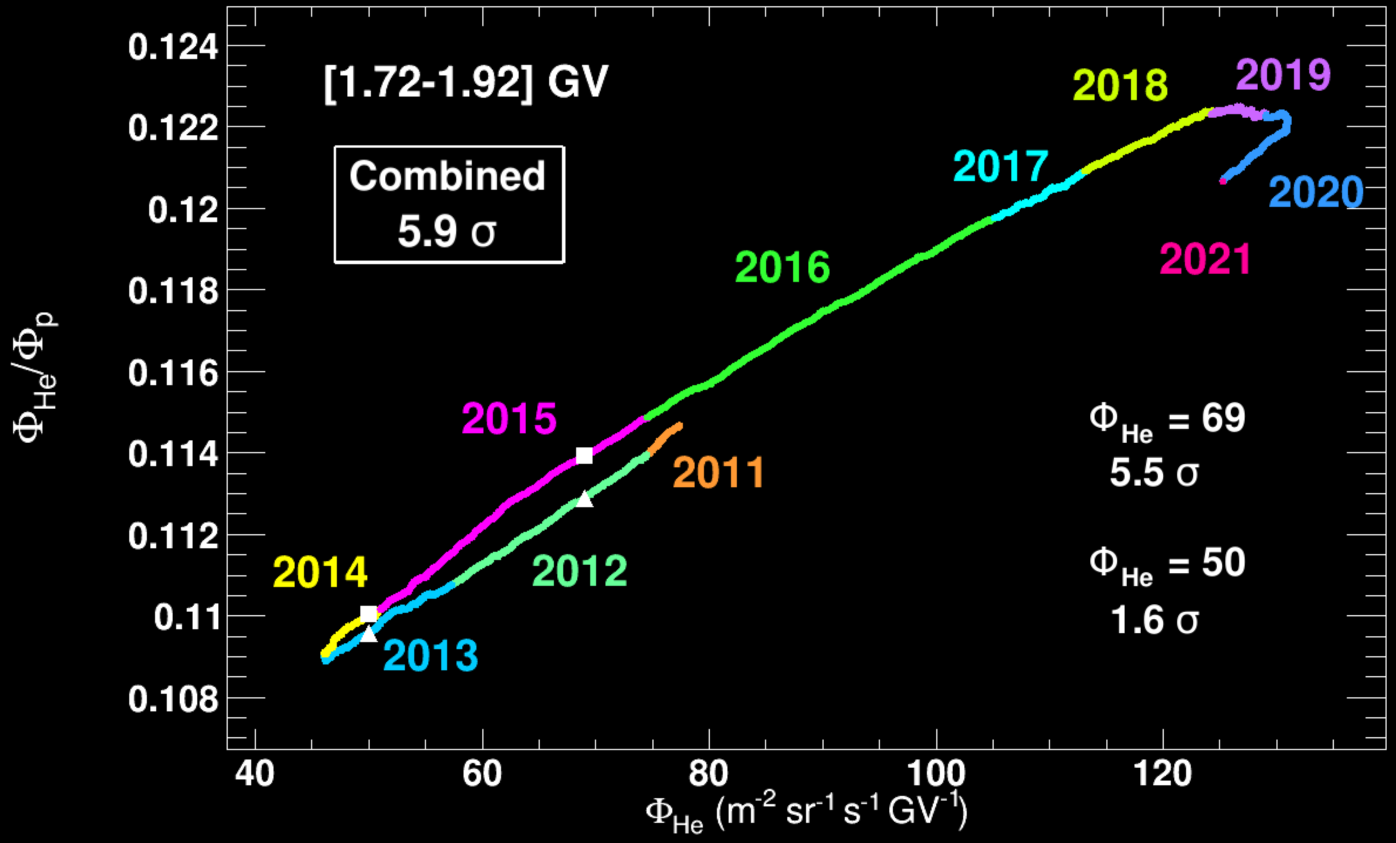

Hysteresis between He/p Flux Ratio and He Flux

The hysteresis is observed with a **significance greater than 7σ**
with combined three rigidity bins below 2.4 GV.

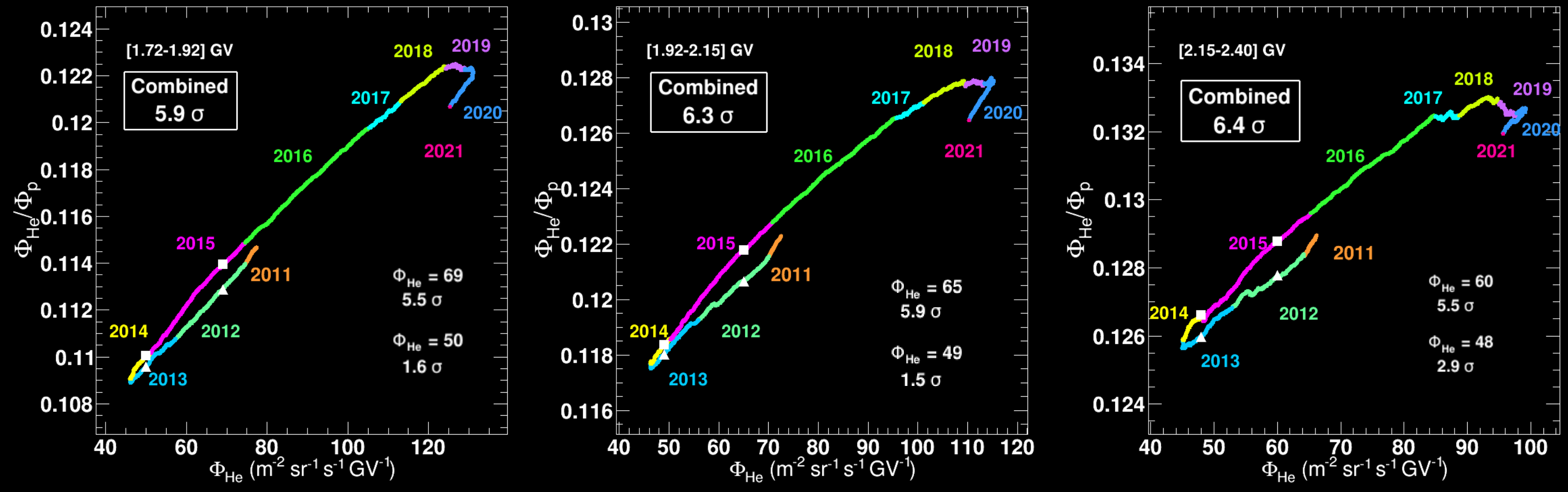

▲ Before solar maximum
■ After solar maximum

The modulation of the helium to proton flux ratio is different before and after the solar maximum in 2014

Hypotheses for He/p time dependent behavior

$$\frac{\partial f}{\partial t} = \underbrace{-\vec{V}_{SW}\cdot\vec{\nabla} f}_{\text{Solar wind convection}} \underbrace{-\vec{V}_{D}\cdot\vec{\nabla} f}_{\boxed{\text{Particle drifts}}} + \underbrace{\vec{\nabla}\cdot(K\cdot\vec{\nabla} f)}_{\boxed{\text{Particle diffusion}}} + \underbrace{\frac{1}{3}\vec{\nabla}\cdot\vec{V}_{SW}\frac{\partial f}{\partial \ln R}}_{\boxed{\text{Adiabatic energy changes}}}$$

Particle convection with the solar wind.

- Particle drifts due to heliospheric magnetic field gradients, curvatures and heliospheric current sheet.
  This term is proportional to the particle velocity (different A/Z → different modulation).

- Particle diffusion due to scattering on magnetic field irregularities.
  This term is proportional to the particle velocity (different A/Z → different modulation).

- Adiabatic energy losses (or gains) due to expansion (or compression) of the solar wind.
  This term is proportional to the particle spectral index (different spectral index → different modulation).